Journal of Nonlinear Modeling and Analysis
Volume 6, Number 2, June 2024, 273–287
http://jnma-online.com
DOI:10.12150/jnma.2024.273

A Novel Numerical Simulations for Fornberg-Whitham and Modified Fornberg-Whitham Equations with Nonhomogeneous Boundary Conditions

İhsan Çelikkaya[1,†]

Abstract In this study, the numerical solutions of the Fornberg-Whitham (FW) equation modeling the qualitative behavior of wave refraction and the modified Fornberg-Whitham (mFW) equation describing the solitary wave and peakon waves with a discontinuous first derivative at the peak have been obtained. To obtain numerical results, the collocation finite element method has been combined with quintic B-spline bases. Although there are solutions to these equations by semi-analytical and analytical methods in the literature, there are very few studies using numerical methods. The stability analysis of the applied method is examined by the von-Neumann Fourier series method. We have considered four test problems with nonhomogeneous boundary conditions that have analytical solutions to show the performance of the method. The numerical results of the two problems are compared with some studies in the literature. Additionally, peakon wave solutions and some new numerical results of the mFW equation, which are not available in the literature, are given in the last two problems. No comparison has been made since there are no numerical results in the literature for the last two problems. The error norms L_2 and L_∞ are calculated to demonstrate the presented numerical scheme's accuracy and efficiency. The advantage of the scheme is that it produces accurate and reliable solutions even for modest values of space and time step lengths, rather than small values that cause excessive data storage in the computation process. In general, large step lengths in the space and time directions result in smaller matrices. This means less storage on the computer and results in faster outcomes. In addition, the present method gives more accurate results than some methods given in the literature.

Keywords Fornberg-Whitham Equation, modified Fornberg-Whitham equation, solitary waves, peakon waves, wind waves, quintic B-spline bases, collocation method

MSC(2010) 65M70, 35G31, 65Z05, 65D05, 65D07, 65L20.

1. Introduction

Numerical methods have become an essential tool for mathematicians and engineers in solving nonlinear partial differential equations in recent years. Traveling wave

[†]the corresponding author.
Email address:ihsan.celikkaya@batman.edu.tr
[1]Department of Mathematics, Batman University, 72070 Batman, Turkey.

solutions constitute an important class of solutions of nonlinear partial differential equations. The Fornberg-Whitham equation, which has a traveling wave solution called the Kink-like wave solution and anti Kink-like solutions, is as follows [1]

$$U_t - U_{xxt} + U_x = UU_{xxx} - UU_x + 3U_xU_{xx}. \tag{1.1}$$

Whitham [2], who studied the qualitative behavior of waves, was the first to propose Eq. (1.1). Fornberg and Whitham [3] obtained a peakon wave solution $U(x,t) = Ae^{-\frac{1}{2}|x-4t/3|}$, where A is a constant. He et al. [4] gave some peakon and solitary wave solutions to the following modified Fornberg-Whitham equation, obtained by taking U^2U_x instead of the nonlinear term UU_x in (1.1):

$$U_t - U_{xxt} + U_x = UU_{xxx} - U^2U_x + 3U_xU_{xx}. \tag{1.2}$$

A notable feature of the mFW equation is that it generates peakon wave solutions. A peakon wave is a wave whose first derivative is discontinuous due to the peaks at its peak. Water covers 71 percent of the earth, and a significant portion of the sun's radiant energy that is not reflected into space is absorbed by the oceans' water. This absorbed energy heats the water, which heats the air above the oceans and creates air currents caused by differences in air temperature. These air currents create wind waves and return some energy to the water. Although the height of the wind waves varies, they reach the shore by traveling long distances [27].

Therefore, it has recently become reasonably interesting to solve numerically and analytically FW and mFW equations, which have many mathematical properties. Marasi and Aqdam [1] used the Homotopy-Pade technique to solve the FW equation. He et al. [4] investigated the mFW equation using bifurcation theory and phase portrait analysis, obtaining some peakons and solitary wave solutions. Dehghan and Heris [5] showed that the variational iteration method and the homotopy perturbation method are powerful and suitable methods for solving the FW equation. Lu [6] used a variational iteration method to solve the FW type equations. Boutarfa et al. [7] obtained the solutions of three types of the FW equations by applying the reproducing kernel Hilbert space method. Hörmann and Okamoto [8] studied spatially periodic solutions of the FW equation to illustrate the mechanism of wave breaking and the formation of shocks for a large class of initial data employing Godunov's finite difference method. Hesam et al. [9] presented a reduced differential transform method for solving FW type equations. Az-Zo'bi [10] implemented the simplest equation method to construct exact traveling-wave solutions to the mFW equation. Li and Song [11] studied the two-component FW equation and obtained the kink-like wave and compacton-like wave solutions. Zhou and Tian [12] utilized the bifurcation method to get traveling wave solutions called kink-like wave solutions and anti kink-like wave solutions for the FW equation. Chen et al. [13] obtained smooth, peaked, and cusped solitary wave solutions of the FW equation under inhomogeneous boundary conditions. Ramadan and Al-luhaibi [14] presented an approximate analytical solution of the nonlinear FW equation using the new iterative method. Abidi and Omrani [15] implemented the variational iteration method and homotopy-perturbation method to solve the nonlinear FW equation analytically. Chen et al. [16] gave some smooth periodic wave, smooth solitary wave, periodic cusp wave, and loop-soliton solutions of the FW equation, and they made some numerical simulations. Biazar and Eslami [17] proposed an analytical method for solving FW type equations based on the homotopy perturbation method. Abidi and Omrani [18] utilized the homotopy analysis method to

approximate the FW equation's analytical solution. Manafian and Lakestani [19] presented a paper in which they used $\tan(\phi/2)$ and $\tanh(\phi/2)$-expansion methods to find the analytical solution of the modified Fornberg-Whitham equation. Ahmad et al. [20] solved the Fornberg–Whitham type equations numerically via the variational iteration algorithm. Shaheen et al. [21] implemented hybrid scheme based on radial basis functions (RBFs) and finite difference to solve nonlinear partial differential equations. Yağmurlu et al. [22] investigated numerical solutions of the modified Fornberg Whitham equation via collocation finite element method using operator splitting.

In this paper, we consider the following initial value problems of the FW and mFW equations with the boundary conditions given by

$$\begin{gathered} U_t - U_{xxt} + U_x = UU_{xxx} - UU_x + 3U_xU_{xx},\ (x,t) \in R \times R^+, \\ U(x,0) = U_0(x), \\ U(a,t) = f_1(t),\ U(b,t) = f_2(t),\ U^{'}(a,t) = f_3(t),\ U^{'}(b,t) = f_4(t), \end{gathered}$$

and

$$\begin{gathered} U_t - U_{xxt} + U_x = UU_{xxx} - U^2U_x + 3U_xU_{xx},\ (x,t) \in R \times R^+, \\ U(x,0) = U_0(x), \\ U(a,t) = f_1(t),\ U(b,t) = f_2(t),\ U^{'}(a,t) = f_3(t),\ U^{'}(b,t) = f_4(t). \end{gathered}$$

2. Quintic B-spline collocation solutions of FW and mFW

Since it is impossible to implement a numerical method on all $x \in R$ and semi-infinite $t \in R^+$, the solution region for a numerical simulation is considered as $a \leq x \leq b$ and $0 \leq t \leq T$. The principal idea of a finite element formulation to get an approximate solution of a physical problem is to result in algebraic equation systems rather than solving differential equations [23, 24]. For this purpose, let x_m be a uniform finite fragmentation of the solution region $[a,b]$, and $a = x_0 < x_1 < ... < x_N = b$ where $m = 0, 1, ..., N$. Taking $h = x_{m+1} - x_m$, $\digamma_m(x)$, $m = -2(1)N+2$,

DOI https://doi.org/10.12150/jnma.2024.273 | Generated on 2024-11-17 05:16:49

quintic B-spline functions on the range $[a,b]$ in terms of nodes x_m as

$$F_m(x)=\frac{1}{h^5}\begin{cases}(x-x_{m-3})^5, & [x_{m-3},x_{m-2}]\\ (x-x_{m-3})^5-6(x-x_{m-2})^5, & [x_{m-2},x_{m-1}]\\ (x-x_{m-3})^5-6(x-x_{m-2})^5+15(x-x_{m-1})^5, & [x_{m-1},x_m]\\ (x-x_{m-3})^5-6(x-x_{m-2})^5+15(x-x_{m-1})^5- & \\ 20(x-x_m)^5, & [x_m,x_{m+1}]\\ (x-x_{m-3})^5-6(x-x_{m-2})^5+15(x-x_{m-1})^5- & \\ 20(x-x_m)^5+ & \\ 15(x-x_{m+1})^5, & [x_{m+1},x_{m+2}]\\ (x-x_{m-3})^5-6(x-x_{m-2})^5+15(x-x_{m-1})^5- & \\ 20(x-x_m)^5+15(x-x_{m+1})^5-6(x-x_{m+2})^5, & [x_{m+2},x_{m+3}]\\ 0, & \text{Otherwise.}\end{cases}$$

The set $\{F_{-2}(x), F_{-1}(x),..., F_{N+1}(x), F_{N+2}(x)\}$ clearly forms a base on the interval $[a,b]$ [25]. The typical element $[x_m,x_{m+1}]$ transforms into the interval $[0,1]$ by using $h\xi = x-x_m$. As shown below, quintic B-spline functions in the range $[0,1]$ can be written in terms of ξ as follows

$$\begin{aligned}F_{m-2}&=1-5\xi+10\xi^2-10\xi^3+5\xi^4-\xi^5,\\ F_{m-1}&=26-50\xi+20\xi^2+20\xi^3-20\xi^4+5\xi^5,\\ F_m&=66-60\xi^2+30\xi^4-10\xi^5,\\ F_{m+1}&=26+50\xi+20\xi^2-20\xi^3-20\xi^4+10\xi^5,\\ F_{m+2}&=1+5\xi+10\xi^2+10\xi^3+5\xi^4-5\xi^5,\\ F_{m+3}&=\xi^5.\end{aligned}\tag{2.1}$$

Thus, the approximate solution on the element $[x_m,x_{m+1}]$ can be written as

$$U_N(x,t)=\sum_{i=m-2}^{m+3}F_i(x)\delta_i(t).$$

The nodal values of $U_N(x,t)$ and its third order derivatives at the nodes x_m are obtained using (2.1) as

$$\begin{aligned}U_N(x_m,t)=U_m&=\delta_{m-2}+26\delta_{m-1}+66\delta_m+26\delta_{m+1}+\delta_{m+2},\\ U_m^{'}&=\frac{5}{h}(-\delta_{m-2}-10\delta_{m-1}+10\delta_{m+1}+\delta_{m+2}),\\ U_m^{''}&=\frac{20}{h^2}(\delta_{m-2}+2\delta_{m-1}-6\delta_m+2\delta_{m+1}+\delta_{m+2}),\\ U_m^{'''}&=\frac{60}{h^3}(-\delta_{m-2}+2\delta_{m-1}-2\delta_{m+1}+\delta_{m+2}).\end{aligned}\tag{2.2}$$

If the expressions given in (2.2) are used in Eq. (1.1), an ordinary differential equation system is obtained as follows

$$\begin{gathered}\overset{\circ}{\delta}_{m-2}+26\overset{\circ}{\delta}_{m-1}+66\overset{\circ}{\delta}_{m}+26\overset{\circ}{\delta}_{m+1}+\overset{\circ}{\delta}_{m+2}-\\ \tfrac{20}{h^2}\left(\overset{\circ}{\delta}_{m-2}+2\overset{\circ}{\delta}_{m-1}-6\overset{\circ}{\delta}_{m}+2\overset{\circ}{\delta}_{m+1}+\overset{\circ}{\delta}_{m+2}\right)+\\ \tfrac{5}{h}\left(-\delta_{m-2}-10\delta_{m-1}+10\delta_{m+1}+\delta_{m+2}\right)+\\ \tfrac{5z_m}{h}\left(-\delta_{m-2}-10\delta_{m-1}+10\delta_{m+1}+\delta_{m+2}\right)-\\ \tfrac{60t_m}{h^2}\left(\delta_{m-2}+2\delta_{m-1}-6\delta_{m}+2\delta_{m+1}+\delta_{m+2}\right)-\\ \tfrac{60z_m}{h^3}\left(-\delta_{m-2}+2\delta_{m-1}-2\delta_{m+1}+\delta_{m+2}\right)=0,\end{gathered} \tag{2.3}$$

where the symbol $\circ$ is the derivative with respect to time and

$$\begin{aligned}U&=z_m=\delta_{m-2}+26\delta_{m-1}+66\delta_m+26\delta_{m+1}+\delta_{m+2},\\ U^2&=(z_m)^2=\left(\delta_{m-2}+26\delta_{m-1}+66\delta_m+26\delta_{m+1}+\delta_{m+2}\right)^2,\\ U_x&=t_m=\frac{5}{h}(-\delta_{m-2}-10\delta_{m-1}+10\delta_{m+1}+\delta_{m+2}).\end{aligned}$$

Instead of the parameters δ_m and $\overset{\circ}{\delta}_m$, $\frac{\delta_m^{n+1}+\delta_m^n}{2}$ Crank-Nicolson and $\frac{\delta_m^{n+1}-\delta_m^n}{\Delta t}$ forward finite difference approaches are written in Eq. (2.3), a recurrence relation between time steps n and $(n+1)$ is obtained as

$$\kappa_1\delta_{m-2}^{n+1}+\kappa_2\delta_{m-1}^{n+1}+\kappa_3\delta_m^{n+1}+\kappa_4\delta_{m+1}^{n+1}+\kappa_5\delta_{m+2}^{n+1}=\kappa_6\delta_{m-2}^{n}+\kappa_7\delta_{m-1}^{n}+\kappa_8\delta_m^{n}+\kappa_9\delta_{m+1}^{n}+\kappa_{10}\delta_{m+2}^{n}, \tag{2.4}$$

where

$$\begin{aligned}\kappa_1&=1-\frac{20}{h^2}-\frac{5\Delta t}{2h}-\frac{5z_m\Delta t}{2h}-\frac{30t_m\Delta t}{h^2}+\frac{30z_m\Delta t}{h^3},\\ \kappa_2&=26-\frac{40}{h^2}-\frac{25\Delta t}{h}-\frac{25z_m\Delta t}{h}-\frac{60t_m\Delta t}{h^2}-\frac{60z_m\Delta t}{h^3},\\ \kappa_3&=66+\frac{120}{h^2}+\frac{180t_m\Delta t}{h^2},\quad \kappa_4=26-\frac{40}{h^2}+\frac{25\Delta t}{h}+\frac{25z_m\Delta t}{h}-\frac{60t_m\Delta t}{h^2}+\frac{60z_m\Delta t}{h^3},\\ \kappa_5&=1-\frac{20}{h^2}+\frac{5\Delta t}{2h}+\frac{5z_m\Delta t}{2h}-\frac{30t_m\Delta t}{h^2}-\frac{30z_m\Delta t}{h^3},\\ \kappa_6&=1-\frac{20}{h^2}+\frac{5\Delta t}{2h}+\frac{5z_m\Delta t}{2h}+\frac{30t_m\Delta t}{h^2}-\frac{30z_m\Delta t}{h^3},\\ \kappa_7&=26-\frac{40}{h^2}+\frac{25\Delta t}{h}+\frac{25z_m\Delta t}{h}+\frac{60t_m\Delta t}{h^2}+\frac{60z_m\Delta t}{h^3},\ \kappa_8=66+\frac{120}{h^2}-\frac{180t_m\Delta t}{h^2},\\ \kappa_9&=26-\frac{40}{h^2}-\frac{25\Delta t}{h}-\frac{25z_m\Delta t}{h}+\frac{60t_m\Delta t}{h^2}-\frac{60z_m\Delta t}{h^3},\\ \kappa_{10}&=1-\frac{20}{h^2}-\frac{5\Delta t}{2h}-\frac{5z_m\Delta t}{2h}+\frac{30t_m\Delta t}{h^2}+\frac{30z_m\Delta t}{h^3}.\end{aligned}$$

The algebraic equation system (2.4) contains $(N+1)$ equations and $(N+5)$ time-dependent parameters $\delta_m(t)$, $m=0(1)N$. To obtain a unique solution for this system, using boundary conditions results in the elimination of the parameters δ_{-2}, δ_{-1}, δ_{N+1} and δ_{N+2}. If the approaches U_m and $U_m^{'}$ are used to transform system

DOI https://doi.org/10.12150/jnma.2024.273 | Generated on 2024-11-17 05:16:49

(2.4) into an $(N+1)\times(N+1)$ pentadiagonal system, the following relations are obtained for the parameters δ_{-2}, δ_{-1}, δ_{N+1} and δ_{N+2}

$$\begin{aligned}
\delta_{-2} &= \frac{165}{4}\delta_0 + \frac{65}{2}\delta_1 + \frac{9}{4}\delta_2 - (5U(a,t) + \frac{13hU^{'}(a,t)}{5})/8,\\
\delta_{-1} &= -\frac{33}{8}\delta_0 - \frac{9}{4}\delta_1 - \frac{1}{8}\delta_2 + (U(a,t) + \frac{hU^{'}(a,t)}{5})/16,\\
\delta_{N+1} &= -\frac{1}{8}\delta_{N-2} - \frac{9}{4}\delta_{N-1} - \frac{33}{8}\delta_N - (U(b,t) - \frac{hU^{'}(a,t)}{5})/16,\\
\delta_{N+2} &= \frac{9}{4}\delta_{N-2} + \frac{65}{2}\delta_{N-1} + \frac{165}{4}\delta_N - (5U(b,t) - \frac{13hU^{'}(b,t)}{5})/8.
\end{aligned}$$

To start the solution of the system (2.4), it is necessary to find the initial vector $\boldsymbol{\delta}_m^0$. Similar to the preceding, the initial vector is generated from the solution of the below matrix system after finding relations for δ_{-2}, δ_{-1}, δ_{N+1} and δ_{N+2} with the help of $U_m^{'}$ and $U_m^{''}$.

$$\begin{bmatrix}
54 & 60 & 6 & & & & & \\
25.5 & 67.5 & 26.25 & 1 & & & & \\
1 & 26 & 66 & 26 & 1 & & & \\
 & & & \ddots & & & & \\
 & & 1 & 26 & 66 & 26 & 1 & \\
 & & & 1 & 26.25 & 67.5 & 25.5 & \\
 & & & & 6 & 60 & 54 &
\end{bmatrix}
\begin{bmatrix} \delta_0^0 \\ \delta_1^0 \\ \delta_2^0 \\ \vdots \\ \delta_{N-2}^0 \\ \delta_{N-1}^0 \\ \delta_N^0 \end{bmatrix}
=
\begin{bmatrix} U_0 \\ U_1 \\ U_2 \\ \vdots \\ U_{N-2} \\ U_{N-1} \\ U_N \end{bmatrix}
+
\begin{bmatrix} (6hU^{'}(a,0) + h^2U^{''}(a,0))/10 \\ (\frac{hU^{'}(a,0)}{5} + \frac{h^2U^{''}(a,0)}{20})/8 \\ \\ \\ \\ \\ -(\frac{hU^{'}(b,0)}{5} - \frac{h^2U^{''}(b,0)}{20})/8 \\ -(6hU^{'}(b,0) - h^2U^{''}(b,0))/10. \end{bmatrix}$$

2.1. Stability analysis

The Von Neumann Fourier series method [26] was used to examine the stability analysis of the system (2.4). In this method, $\delta_m^n = \xi^n e^{i\beta mh}$ is taken, where $i=\sqrt{-1}$, β is mode number, ξ is the amplification factor, and h is the space step. Since this method is valid for linear schemes, ρ and σ constants are taken instead of z_m and w_m, respectively. If $\delta_m^n = \xi^n e^{i\beta mh}$ is written in the system (2.4) and if necessary operations are carried out, the following expressions are obtained

$$\frac{\xi(t^{n+1})}{\xi(t^n)} = \frac{\kappa_6 e^{-2i\beta h} + \kappa_7 e^{-i\beta h} + \kappa_8 + \kappa_9 e^{i\beta h} + \kappa_{10} e^{2i\beta h}}{\kappa_1 e^{-2i\beta h} + \kappa_2 e^{-i\beta h} + \kappa_3 + \kappa_4 e^{i\beta h} + \kappa_5 e^{2i\beta h}}$$

or

$$\begin{aligned}
\frac{\xi(t^{n+1})}{\xi(t^n)} &= \frac{[(\kappa_6+\kappa_{10})\cos(2\beta h)+(\kappa_7+\kappa_9)\cos(\beta h)+\kappa_8]+i[(\kappa_{10}-\kappa_6)\sin(2\beta h)+(\kappa_9-\kappa_7)\sin(\beta h)]}{[(\kappa_1+\kappa_5)\cos(2\beta h)+(\kappa_2+\kappa_4)\cos(\beta h)+\kappa_3]+i[(\kappa_5-\kappa_1)\sin(2\beta h)+(\kappa_4-\kappa_2)\sin(\beta h)]}\\
&= \frac{K+iL}{M+iN}
\end{aligned}$$

where

$$\begin{aligned}
K &= [(\kappa_6+\kappa_{10})\cos(2\beta h)+(\kappa_7+\kappa_9)\cos(\beta h)+\kappa_8],\\
L &= [(\kappa_{10}-\kappa_6)\sin(2\beta h)+(\kappa_9-\kappa_7)\sin(\beta h)],\\
M &= [(\kappa_1+\kappa_5)\cos(2\beta h)+(\kappa_2+\kappa_4)\cos(\beta h)+\kappa_3],\\
N &= [(\kappa_5-\kappa_1)\sin(2\beta h)+(\kappa_4-\kappa_2)\sin(\beta h)].
\end{aligned}$$

The condition $\left|\frac{\xi(t^{n+1})}{\xi(t^n)}\right| \leq 1$ must be satisfied for the method to be stable. Specifically, the inequality $\left|K^2\right| + \left|L^2\right| \leq \left|M^2\right| + \left|N^2\right|$ must be maintained. Thus, the following expression is obtained

$$\left|K^2\right|+\left|L^2\right|-\left|M^2\right|-\left|N^2\right|=\frac{1920\Delta t\sigma(\cos^2\beta h+\cos\beta h-2)[\cos\beta h(h^2\cos\beta h+13h^2-20\cos\beta h-20)+16h^2+40]}{h^4} \leq 0.$$

The method is unconditionally stable since $\left|K^2\right|+\left|L^2\right|-\left|M^2\right|-\left|N^2\right| \leq 0$. Besides, it should still be taken into account that the solutions are not distorted when choosing h and Δt.

3. Numerical applications

In this section, four test problems have been considered for the numerical simulations. To confirm the accuracy and efficiency of the proposed method, we have calculated the error norms L_2 and L_∞ that measure the difference between exact (U) and numerical (U_N) solutions given as follows

$$L_2 = \sqrt{h\sum_{j=0}^{N}\left|U(x_j,t)-U_N(x_j,t)\right|^2},\ L_\infty = \max_{0\leq j\leq N}\left|U(x_j,t)-U_N(x_j,t)\right|.$$

The boundary conditions for all the problems given below are taken from the exact solution of the problems.

Problem 1. Consider the Fornberg-Whitham equation

$$U_t - U_{xxt} + U_x = UU_{xxx} - UU_x + 3U_xU_{xx}.$$

The exact solution of the equation is [18]

$$U(x,t) = \exp\left(\frac{x}{2} - \frac{2t}{3}\right).$$

The problem's initial condition can be found as $U_0(x,0) = \exp(x/2)$ by taking $t = 0$ in the exact solution. As can be seen from the exact solution, the problem has nonhomogeneous boundary conditions. Table 1 shows the error norms L_2 and L_∞ calculated at different times for various values of Δt and $h = 0.1,\ 0.05$, $-5 \leq x \leq 5$. It can be seen from the table that the error norms L_2 and L_∞ are sufficiently small, and both errors decrease as Δt decreases with increasing time t. Table 2 provides a comparison of absolute errors at various x and t. It is seen from the table that the absolute errors obtained with our method are considerably smaller than those of Ref. [18], which is evident in the efficiency of the present numerical scheme given by Eq. (2.4). It is seen from Figure 1 that the approximate and exact solutions are in good harmony, and the error increases towards the right border at $t = 1$. In Table 3, it is obvious that the absolute errors obtained by the finite element method at $t = 5$ are smaller than those in Ref. [14, 18] and the numerical solutions are closer to the exact solution.

Problem 2. As for the second problem, we consider the modified Fornberg-Whitham equation

$$U_t - U_{xxt} + U_x = UU_{xxx} - U^2U_x + 3U_xU_{xx}.$$

Table 1. The error norms L_2 and L_∞ for $h = 0.1$, 0.05 over $-5 \leq x \leq 5$ of Problem 1.

		$\Delta t = 0.01$		$\Delta t = 0.001$		$\Delta t = 0.0001$	
h	t	L_2	L_∞	L_2	L_∞	L_2	L_∞
0.1	0.2	0.3412E-3	0.5154E-3	0.3242E-4	0.4825E-4	0.3226E-5	0.4795E-5
	0.4	0.3298E-3	0.4753E-3	0.3159E-4	0.4471E-4	0.3146E-5	0.4444E-5
	0.6	0.2973E-3	0.4217E-3	0.2862E-4	0.3997E-4	0.2852E-5	0.3974E-5
	0.8	0.2643E-3	0.3713E-3	0.2560E-4	0.3512E-4	0.2553E-5	0.3493E-5
	1	0.2344E-3	0.3284E-3	0.2276E-4	0.3118E-4	0.2271E-5	0.3101E-5
0.05	0.2	0.1859E-3	0.2945E-3	0.1672E-4	0.2571E-4	0.1654E-5	0.2538E-5
	0.4	0.1774E-3	0.2696E-3	0.1625E-4	0.2362E-4	0.1611E-5	0.2332E-5
	0.6	0.1579E-3	0.2384E-3	0.1471E-4	0.2104E-4	0.1460E-5	0.2078E-5
	0.8	0.1395E-3	0.2094E-3	0.1314E-4	0.1857E-4	0.1305E-5	0.1835E-5
	1	0.1231E-3	0.1840E-3	0.1168E-4	0.1640E-4	0.1161E-5	0.1621E-5

Table 2. Comparison of absolute error at different points and time for $h = 0.05$, $\Delta t = 0.0001$ over $-5 \leq x \leq 5$ of Problem 1.

	x/t	0.2	0.4	0.6	0.8	1
Present	-4	0.19061E-9	0.24008E-9	0.59222E-9	0.17926E-8	0.47527E-8
	-2	0.27838E-8	0.32590E-8	0.30907E-8	0.27694E-8	0.26393E-8
	0	0.21033E-7	0.25658E-7	0.25437E-7	0.42710E-8	0.87626E-7
	2	0.12087E-6	0.11890E-6	0.10770E-6	0.10258E-6	0.94021E-7
	4	0.83881E-7	0.44127E-7	0.31491E-7	0.26988E-7	0.22057E-7
[18]	-4	2.22193E-5	9.47416E-6	4.83886E-5	6.71560E-5	5.36314E-5
	-2	6.03987E-5	2.57532E-5	1.31533E-4	1.82549E-4	1.45785E-4
	0	1.64180E-5	7.00049E-5	3.57546E-4	4.96219E-4	3.96285E-4
	2	4.46289E-4	1.90293E-4	9.71910E-4	1.34886E-3	1.07721E-3
	4	1.21314E-4	5.17269E-4	2.64192E-3	3.66659E-3	2.92817E-3

Table 3. Comparison of some nodal values and absolute errors at $t = 5$ for $h = 0.05$ and $\Delta t = 0.0001$ over $-5 \leq x \leq 5$ of Problem 1.

			Absolute Errors		
x	U_{exact}	$U_{present}$	Present	[14](NIM)	[18]($\hbar = -1.01$)
-4	0.0048279500	0.0048255274	0.24226E-5	1.65602E-3	4.73109E-5
-2	0.0131237287	0.0131228885	0.84023E-6	4.50155E-3	1.28604E-4
0	0.0356739933	0.0356737902	0.20313E-6	1.22364E-2	3.49584E-4
2	0.0969719679	0.0969719599	0.80098E-8	3.32622E-2	9.50270E-4
4	0.2635971381	0.2635971667	0.28600E-7	9.04161E-2	2.58313E-3

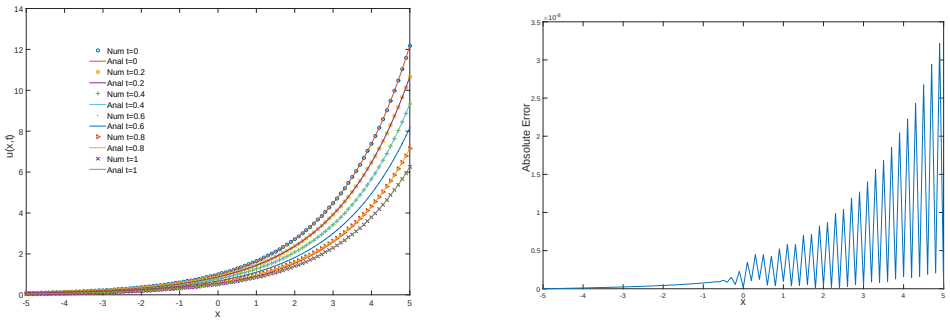

Figure 1. Solution curves (Left) of Problem 1 for $h = 0.1$, $\Delta t = 0.000001$ at different times and error graph (Right) at $t = 1$.

DOI https://doi.org/10.12150/jnma.2024.273 | Generated on 2024-11-17 05:16:49

Table 4. The error norms L_2 and L_∞ for various h and Δt of Problem 2.

$\Delta t = 0.001,\ -10 \le x \le 10$						
	$h = 0.1$		$h = 0.025$		$h = 0.0125$	
t	L_2	L_∞	L_2	L_∞	L_2	L_∞
0.02	2.7661E-7	3.6479E-7	0.7345E-7	1.0466E-7	0.3757E-7	0.5395E-7
0.04	5.5428E-7	7.2726E-7	1.4858E-7	2.0957E-7	0.7594E-7	1.0689E-7
0.06	8.3252E-7	1.0867E-6	2.2409E-7	3.1249E-7	1.1367E-7	1.5891E-7
0.08	1.1109E-6	1.4426E-6	2.9916E-7	4.1189E-7	1.5019E-7	2.2348E-7
0.1	1.3890E-6	1.7944E-6	3.7329E-7	5.0671E-7	1.8531E-7	2.9161E-7
$h = 0.025,\ -40 \le x \le 40$						
	$\Delta t = 0.1$		$\Delta t = 0.001$		$\Delta t = 0.0001$	
t	L_2	L_∞	L_2	L_∞	L_2	L_∞
2	0.1117E-3	0.4434E-4	0.1117E-7	0.4428E-8	0.1201E-9	0.4523E-10
4	0.2229E-3	0.9020E-4	0.2228E-7	0.9012E-8	0.2500E-9	0.9813E-10
6	0.3326E-3	0.1349E-3	0.3327E-7	0.1348E-7	0.3763E-9	0.1471E-9
8	0.4405E-3	0.1771E-3	0.4408E-7	0.1771E-7	0.4995E-9	0.1926E-9
10	0.5463E-3	0.2168E-3	0.5467E-7	0.2168E-7	0.6208E-9	0.2417E-9

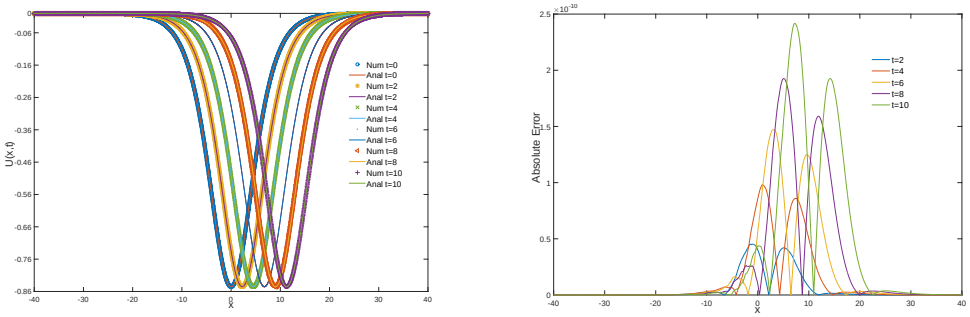

Figure 2. The wave profiles (Left) and the absolute errors (Right) for $h = 0.025$, $\Delta t = 0.0001$ at different times of Problem 2.

The exact solitary wave solution of the equation is [4]

$$U(x,t) = \frac{3}{4}\left(\sqrt{15} - 5\right) \sec h^2 \left(c(x - (5 - \sqrt{15})t)\right),$$

where $c = \sqrt{10(5 - \sqrt{15})}/20$ is a constant, and the initial condition can be obtained from the exact solution for $t = 0$. For this problem, the calculated error norms L_2 and L_∞ for $\Delta t = 0.001$, $-10 \le x \le 10$ and $h = 0.025$, $-40 \le x \le 40$ are displayed in Table 4. It is seen from table that the error norms L_2 and L_∞ are sufficiently small enough, and both errors decrease as h and Δt decrease. Some nodal values of $U_N(x,t)$ are given in Table 5. It is seen from the Table 5 that the numerical solutions obtained by the present method converge to the exact solution. Furthermore, although absolute errors are given for the right side of the solution region in study Ref. [6, 7], we have given some new results for the left side of the solution region too. It is seen that the absolute errors calculated by the presented method are smaller than those in the Refs. [6, 7]. In Table 6, the solution region has been chosen as $[-6, 6]$ and some nodal values have been given for different x, t and the absolute errors have been compared with the results in Ref. [17]. In Figure 2, it is obvious that the waves move to the right as time progresses, and the greatest absolute error is at the points near the peak of the waves. The amplitude of the wave at $x = 0$ for $t = 0$ is -0.8452624903, while the value of the amplitude at position $x = 11.20$ for $t = 10$ is -0.84514524871, its approximate value is calculated

DOI https://doi.org/10.12150/jnma.2024.273 | Generated on 2024-11-17 05:16:49

Table 5. Comparison of some nodal values and absolute errors for $h = 0.0125$ and $\Delta t = 0.001$ over $-10 \leq x \leq 10$ of Problem 2.

	x/t	0.02	0.04	0.06	0.08	0.1
	−10	-0.109211848	-0.108443189	-0.107679544	-0.106920887	-0.106167190
	−7.5	-0.231961916	-0.230470676	-0.228987236	-0.227511580	-0.226043691
	−5	-0.445829237	-0.443512811	-0.441201792	-0.438896257	-0.436596279
	−2.5	-0.710149444	-0.707995721	-0.705831602	-0.703657276	-0.701472929
Exact	0	-0.845250391	-0.845214093	-0.845153600	-0.845068921	-0.844960064
	2.5	-0.714424960	-0.716546377	-0.741260458	-0.720755597	-0.722843025
	5	-0.450478005	-0.452810189	-0.455147467	-0.457489755	-0.459836973
	7.5	-0.234967853	-0.236482581	-0.238005167	-0.239535625	-0.241073969
	10	-0.110764319	-0.111548184	-0.112337172	-0.113131310	-0.113930626
	−10	-0.109211842	-0.108443169	-0.107679506	-0.106920826	-0.106167104
	−7.5	-0.231961911	-0.230470667	-0.228987223	-0.227511562	-0.226043668
	−5	-0.445829237	-0.443512810	-0.441201791	-0.438896256	-0.436596277
	−2.5	-0.710149444	-0.707995721	-0.705831602	-0.703657276	-0.701472929
Present	0	-0.845250391	-0.845214093	-0.845153600	-0.845068921	-0.844960064
	2.5	-0.714424960	-0.716546377	-0.718656652	-0.720755597	-0.722843025
	5	-0.450478005	-0.452810189	-0.455147466	-0.457489755	-0.459836973
	7.5	-0.234967853	-0.236482581	-0.238005167	-0.239535625	-0.241073969
	10	-0.110764319	-0.111548184	-0.112337172	-0.113131310	-0.113930626
	−10	$0.58984E$-8	$0.19777E$-7	$0.38494E$-7	$0.60664E$-7	$0.85606E$-7
	−7.5	$0.44450E$-8	$0.90688E$-8	$0.13702E$-7	$0.18277E$-7	$0.22769E$-7
	−5	$0.34409E$-9	$0.71444E$-9	$0.10977E$-8	$0.14883E$-8	$0.18839E$-8
	−2.5	$0.10605E$-10	$0.18233E$-10	$0.24051E$-10	$0.28045E$-10	$0.30310E$-10
Present	0	$0.198708E$-11	$0.369504E$-11	$0.41350E$-11	$0.42804E$-11	$0.36213E$-11
	2.5	$0.41820E$-10	$0.83262E$-10	$0.12455E$-9	$0.16557E$-9	$0.20631E$-9
	5	$0.27421E$-10	$0.55146E$-10	$0.83257E$-10	$0.11140E$-9	$0.13877E$-9
	7.5	$0.59104E$-11	$0.11049E$-10	$0.13932E$-10	$0.10890E$-10	$0.72232E$-11
	10	$0.60040E$-11	$0.33428E$-10	$0.11037E$-9	$0.30575E$-9	$0.78960E$-9
	2.5	$2.45E$-8	$4.90E$-8	$1.96E$-8	$3.70E$-8	$4.2E$-9
[7]	5	$8.36E$-8	$6.4E$-9	$4.E$-10	$4.76E$-8	$7.11E$-8
	7.5	$1.86E$-8	$7.09E$-8	$6.0E$-9	$7.06E$-8	$4.98E$-8
	10	$6.82E$-8	$7.9E$-9	$5.21E$-8	$9.83E$-8	$1.23E$-8
	2.5	$1.180E$-4	$2.363E$-4	$3.547E$-4	$4.731E$-4	$5.914E$-4
	5	$2.124E$-5	$4.797E$-5	$8.029E$-5	$1.183E$-4	$1.622E$-4
[6]	7.5	$2.805E$-5	$5.772E$-5	$8.902E$-5	$1.220E$-4	$1.565E$-4
	10	$5.528E$-6	$1.084E$-5	$1.591E$-5	$2.071E$-5	$2.524E$-5

Table 6. Some nodal values and comparison of absolute errors for $h = 0.1$ and $\Delta t = 0.0001$ over $-6 \leq x \leq 6$ of Problem 2.

		$\lvert U_{Num} - U_{Anal}\rvert$	$\lvert U_{Num} - U_{Anal}\rvert$	Numerical	Analytical
x	t	[17]	Present		
1	0.03	$2.015219E$-4	$0.805070E$-8	−0.8234141827	−0.823414191
1	0.1	$1.803436E$-4	$3.286102E$-8	−0.826786293	−0.826786326
2	0.04	$1.626634E$-4	$0.417141E$-8	−0.760402313	−0.760402318
3	0.05	$1.081287E$-3	$0.204781E$-8	−0.668366805	−0.668366807
5	0.02	$1.949816E$-4	$0.121802E$-9	−0.450478005	−0.450478005
5	0.08	$1.012877E$-2	$0.589629E$-9	−0.457489755	−0.457489755
6	0.06	$9.963555E$-4	$0.298929E$-10	−0.357274222	−0.357274222
−1	0.03	$2.163505E$-4	$5.747642E$-8	−0.820311546	−0.820311603
−1	0.1	$1.166166E$-3	$2.178465E$-7	−0.816448453	−0.816448670
−2	0.04	$3.30110E$-5	$2.084454E$-7	−0.752989657	−0.752989865
−3	0.05	$4.186843E$-4	$7.030596E$-7	−0.656712461	−0.656713164
−5	0.02	$2.222605E$-4	$1.974517E$-6	−0.445827263	−0.445829237
−5	0.08	$3.857237E$-3	$8.055728E$-6	−0.438888201	−0.438896257
−6	0.06	$1.254387E$-3	$6.257651E$-5	−0.345022485	−0.345085061

DOI https://doi.org/10.12150/jnma.2024.273 | Generated on 2024-11-17 05:16:49

Table 7. The error norms L_2 and L_∞ for $h = 0.05$ and $\Delta t = 0.001$ over $-40 \leq x \leq 40$ and the maximum amplitude and positions of the waves for Problem 3.

t	L_2	L_∞	x_{Present}	Present	x_{Exact}	Exact
0.0	0	0	0.00	1.0717967697	0.00	1.0717967697
0.1	3.427711E-3	5.799864E-3	0.10	1.0641940415	0.10	1.0677405597
0.2	4.443314E-3	5.424758E-3	0.20	1.0614210850	0.20	1.0637027426
0.3	5.085654E-3	5.152561E-3	0.30	1.0592301893	0.30	1.0596832076
0.4	5.564875E-3	6.959314E-3	0.40	1.0570739402	0.45	1.0598271873
0.5	5.991543E-3	9.519186E-3	0.50	1.0547586108	0.55	1.0638473767
0.6	6.434189E-3	1.248082E-2	0.65	1.0554050293	0.65	1.0678858521
0.7	6.905057E-3	1.559166E-2	0.75	1.0560591819	0.75	1.071650839
0.8	6.611694E-3	1.132711E-2	0.85	1.0562681827	0.85	1.0675952910
0.9	6.477428E-3	7.535795E-3	0.95	1.0560223372	0.95	1.063558132
1.0	6.487581E-3	8.363858E-3	1.05	1.0553225848	1.05	1.0595392513
1.1	6.629316E-3	1.026466E-2	0.15	1.0541790970	1.20	1.0599711904
1.2	6.909973E-3	1.257378E-2	1.25	1.0526101073	1.30	1.0639920344
1.3	7.430852E-3	1.531826E-2	1.40	1.0527129076	1.40	1.0680311683
1.4	8.676064E-3	1.793483E-2	1.50	1.0535701045	1.50	1.0715049317

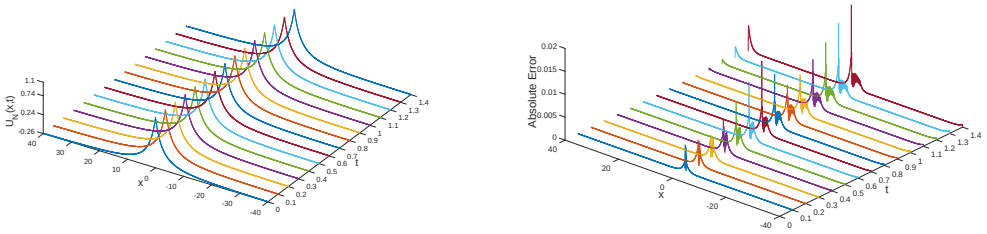

Figure 3. The physical behavior of peakon waves (Left) and absolute errors (Right) for $h = 0.05$ and $\Delta t = 0.001$ at different times over $-40 \leq x \leq 40$ of Problem 3.

as -0.84514525926.

Problem 3. In the third problem, the peakon solutions of the modified Fornberg-Whitham equation have been obtained numerically. One of the peakon solutions of the modified Fornberg-Whitham equation is [4]

$$U(x,t) = \left(\sqrt{3}-2\right) + \frac{1}{\left(\frac{1}{\sqrt{5(2-\sqrt{3})}} + \frac{\sqrt{30}}{30}\left|x - 4(2-\sqrt{3})t\right|\right)^2}.$$

The initial condition can be obtained by writing $t = 0$ in the function $U(x,t)$. Since there are no numerical results in the literature regarding this exact solution of the mFW equation, no comparisons have been made. Therefore, some physical properties of the mFW equation have been investigated, and some numerical results have been given under some conditions. The maximum heights and positions of the peakon waves, as well as the error norms L_2 and L_∞ at different times for $h = 0.05$ and $\Delta t = 0.001$, are given in Table 7. The reason for the considerable error norm L_∞ is that the peakon wave peak is sharp, and all these errors occur at the positions where the peak is located. It is also seen in Figure 3 (Right) that the maximum absolute error calculated at each time is at its peak. Also, Figure 3 (Left) shows that peakon waves move to the right as time progresses.

Problem 4. In the fourth and last problem, two different travelling wave

DOI https://doi.org/10.12150/jnma.2024.273 | Generated on 2024-11-17 05:16:49

Table 8. The error norms L_2 and L_∞ for $h = 0.4$ and $\Delta t = 0.01$, 0.001 at different times over $-50 \le x \le 50$, and maximum wave heights and positions of $U_1(x,t)$ for Problem 4.

Δt	t	L_2	L_∞	x	Present	Exact
0.01	0	0	0	−26.80	−0.845199750	−0.845199750
	10	0.390083E-5	0.144941E-5	−15.60	−0.8449109626	−0.8449110475
	20	0.754750E-5	0.272711E-5	−4.40	−0.8443880247	−0.8443882517
	30	1.089308E-5	0.380747E-5	7.20	−0.8448071230	−0.8448079745
	40	1.400909E-5	0.477147E-5	18.40	−0.8451514287	−0.8451523574
	50	1.696385E-5	0.566480E-5	29.60	−0.8452614640	−0.8452623792
0.001	10	0.160189E-5	0.069454E-5	−15.60	−0.8449112481	−0.8449110475
	20	0.283469E-5	0.110580E-5	−4.40	−0.8443885219	−0.8443882517
	30	0.390897E-5	0.144257E-5	7.20	−0.8448084591	−0.8448079745
	40	0.490351E-5	0.174919E-5	18.40	−0.8451528625	−0.8451523574
	50	0.585437E-5	0.204232E-5	29.60	−0.8452628727	−0.8452623792

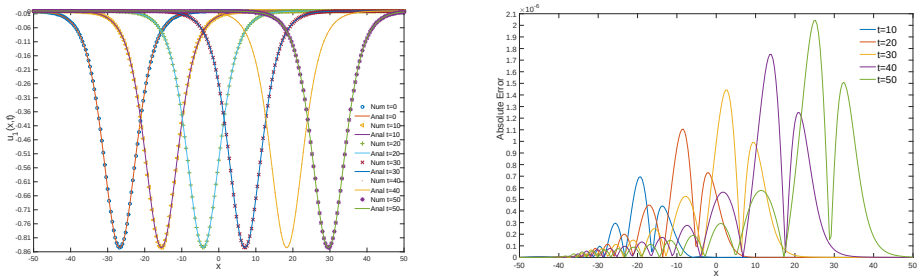

Figure 4. The wave profiles (Left) and absolute errors (Right) of $U_1(x,t)$ for $h = 0.4$, $\Delta t = 0.001$ at different times of Problem 4.

solutions of the modified Fornberg-Whitham equation are obtained numerically by the present method. The modified Fornberg-Whitham equation has the following exact travelling wave solutions [10]

$$U_1(x,t) = \frac{30\lambda^2\mu e^{\lambda\left(x-10\lambda^2 t+c\right)}}{\left(1-\mu e^{\lambda(x-10\lambda^2 t+c)}\right)^2} \quad \text{and} \quad U_2(x,t) = -\frac{30\lambda^2\mu e^{\lambda\left(x-10\lambda^2 t+c\right)}}{\left(1+\mu e^{\lambda(x-10\lambda^2 t+c)}\right)^2},$$

where $-c$ controls the wave position while $10\lambda^2$ is the wave velocity. The relations between the constants λ and μ for $U_1(x,t)$ and $U_2(x,t)$ are $\lambda = -\mu = \sqrt{0.5-\sqrt{0.15}}$ and $\lambda = -\mu = -\sqrt{0.5-\sqrt{0.15}}$, respectively. Numerical solutions of the mFW equation are not available in the literature for exact solutions U_1 and U_2. For this reason, no comparison has been made, and the numerical solutions of the equation have been examined.

L_2 and L_∞ error norms, as well as maximum wave amplitudes and their positions, are calculated in Tables 8 and 9 for functions $U_1(x,t)$ and $U_2(x,t)$, respectively. When one looks at these tables, it is seen that as Δt decreases, the error norms also decrease. The graphs of solitary waves corresponding to $U_1(x,t)$ and $U_2(x,t)$ and their absolute errors at different times are shown in Figures 4 and 5, respectively. It is seen from the figures that the waves move to the right as time progresses, and the wave bandwidth corresponding to $U_1(x,t)$ is wider than $U_2(x,t)$.

Table 9. The error norms L_2 and L_∞ for $h = 0.2$ and $\Delta t = 0.001$, 0.0001 over $-50 < x < 50$, and maximum wave heights and positions at different times of $U_2(x,t)$ for Problem 4.

Δt	t	L_2	L_∞	x	Present	Exact
	0	0	0	−20.00	−6.6487942340	−6.6487942340
	0.5	0.723671E-3	0.371612E-3	−15.60	−6.6536553745	−6.6536631734
	1	1.421725E-3	0.730242E-3	−11.20	−6.6546197491	−6.6546039255
	1.5	2.098968E-3	1.077213E-3	−6.80	−6.6516853194	−6.6516142683
0.001	2	2.757376E-3	1.411994E-3	−2.40	−6.6448600020	−6.6447012614
	2.5	3.399565E-3	1.828694E-3	2.20	−6.6448387619	−6.6450587551
	3	5.078002E-3	4.108085E-3	6.60	−6.6502954245	−6.6518124631
	0.5	0.108751E-3	0.063875E-3	−15.60	−6.6536736880	−6.6536631734
	1	0.190161E-3	0.104984E-3	−11.20	−6.6546117969	−6.6546039255
	1.5	0.270125E-3	0.146798E-3	−6.80	−6.6516156346	−6.6516142683
0.0001	2	0.350582E-3	0.191292E-3	−2.40	−6.6446949823	−6.6447012614
	2.5	0.452276E-3	0.307201E-3	2.20	−6.6450284645	−6.6450587551
	3	3.392168E-3	2.364555E-3	6.60	−6.6504870065	−6.6518124631

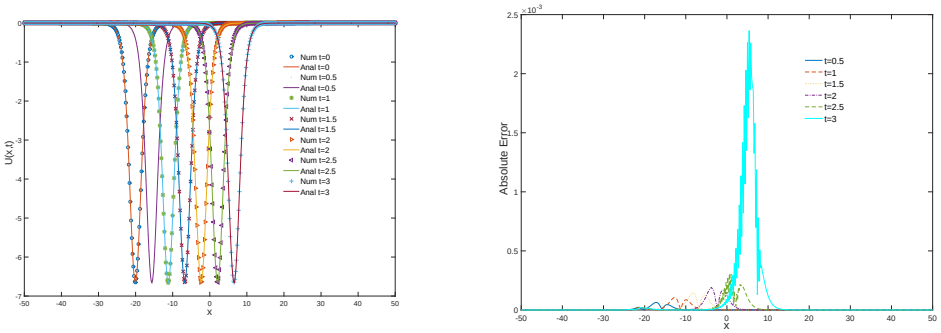

Figure 5. The wave profiles (Left) and absolute errors (Right) of $U_2(x,t)$ for $h = 0.2$ and $\Delta t = 0.0001$ at different times of Problem 4.

4. Conclusions

In this study, numerical solutions of FW and mFW equations with strong nonlinearity have been obtained by the collocation method using quintic B-spline bases. In addition, some numerical results that are not previously available in the literature for the mFW equation are calculated, and the physical properties of the solution is investigated. The method's effectiveness and powerfulness have been demonstrated by calculating the error norms L_2 and L_∞, which are frequently used in the literature. We discovered that our results are completely satisfactory, despite the fact that a very small h is not used to calculate numerical results. As a result of the calculations, it has been seen that the finite element method gave more convergent results than methods such as the variational iteration method (VIM), homotopy perturbation method (HPM), and the homotopy analysis method (HAM). Thus, the proposed method can be considered as a suitable method for modeling various wave phenomena and effectively solving numerous nonlinear partial differential equations arising in various fields of physics, engineering, and applied mathematics.

References

[1] H.R. Marasi and A. P. Aqdam, *Homotopy analysis method and homotopy Padè approximants for solving the Fornberg-Whitham equation*, Eurasian Mathematical journal, 2015, 6(1), 65-75.

[2] G. B. Whitham, *Variational methods and applications to water waves*, Pro-

DOI https://doi.org/10.12150/jnma.2024.273 | Generated on 2024-11-17 05:16:49

ceedings of the Royal Society of London. Series A, Mathematical and Physical Sciences, 1967, 299, 6-25.

[3] B. Fornberg and G.B. Whitham, *A numerical and theoretical study of certain nonlinear wave phenomena*, Philosophical Transactions of the Royal Society of London. Series A, Mathematical and Physical Sciences, 1978, 289, 373-404.

[4] B. He, Q. Meng and S. Li, *Explicit peakon and solitary wave solutions for the modified Fornberg-Whitham equation*, Applied Mathematics and Computation, 2010, 217(5), 1976–1982. doi:10.1016/j.amc.2010.06.05

[5] M. Dehghan and J. M. Heris, *Study of the wave-breaking's qualitative behavior of the Fornberg-Whitham equation via quasi-numeric approaches*,International Journal of Numerical Methods for Heat & Fluid, 2012, 22(5), 537-553. https://doi.org/10.1108/09615531211231235

[6] J. Lu, *An analytical approach to the Fornberg–Whitham type equations by using the variational iteration method*, Computers and Mathematics with Applications, 2011, 61, 2010–2013. doi:10.1016/j.camwa.2010.08.052

[7] B. Boutarfa, A. Akgül and M. Inc, *New approach for the Fornberg-Whitham type equations*, Journal of Computational and Applied Mathematics, 2017, 312, 13-26. http://dx.doi.org/10.1016/j.cam.2015.09.016

[8] G. Hörmann and H. Okamoto, *Weak periodic solutions and numerical case studies of the Fornberg-Whitham equation*, Discrete and Continuous Dynamical Systems, 2019, 39, 4455-4469. doi:10.3934/dcds.2019182

[9] S. Hesam, A. R. Nazemi and A. Haghbin, *Reduced Differential Transform Method for solving the Fornberg-Whitham type equation*, International Journal of Nonlinear Science, 2012, 13(2), 158-162.

[10] E. Az-Zo'bi, *Peakon and Solitary Wave Solutions for The Modified Fornberg-Whitham Equation using Simplest Equation Method*, International Journal of Mathematics and Computer Science, 2019, 14(3), 635-645.

[11] S. Li and M. song, *Kink-Like Wave and Compacton-Like Wave Solutions for a Two-Component Fornberg-Whitham Equation*, Abstract and Applied Analysis, 2014, 2014, 1-13. https://doi.org/10.1155/2014/621918

[12] J. Zhou and L. Tian, *A type of bounded traveling wave solutions for the Fornberg-Whitham equation*, Journal of Mathematical Analysis and Applications, 2008, 346, 255–261. doi:10.1016/j.jmaa.2008.05.055

[13] A. Chen, J. Li and W. Huang, *Single peak solitary wave solutions for the Fornberg-Whitham equation*, Applicable Analysis, 2012, 91(3), 587–600. http://dx.doi.org/10.1080/00036811.2010.550577

[14] M. A. Ramadan and M. S. Al-Luhaibi, *New Iterative Method for Solving the Fornberg-Whitham Equation and Comparison with Homotopy Perturbation Transform Method*, British Journal of Mathematics & Computer Science, 2014, 4(9), 1213-1227.

[15] F. Abidi and K. Omrani, *Numerical solutions for the nonlinear Fornberg-Whitham equation by He's methods*, International Journal of Modern Physics B, 2011, 25, 4721-4732. DOI: 10.1142/S0217979211059516

[16] A. Chen, J. Li, X. Deng and W. Huang, *Travelling wave solutions of the Fornberg-Whitham equation*, Applied Mathematics and Computation, 215:8 (2009) 3068-3075. doi:10.1016/j.amc.2009.09.057

[17] J. Biazar, M. Eslami, Approximate solutions for Fornberg-Whitham type equations, International Journal of Numerical Methods for Heat & Fluid, 2012, 22(6), 803–812. DOI 10.1108/09615531211244934

[18] F. Abidi and K. Omrani, *The homotopy analysis method for solving the Fornberg-Whitham equation and comparison with Adomian's decomposition method*, Computers and Mathematics with Applications, 2010, 59(8), 2743-2750. doi:10.1016/j.camwa.2010.01.042

[19] J. Manafian and M. Lakestani, *The Classification of the Single Traveling-Wave Solutions to the Modified Fornberg-Whitham Equation*, International Journal of Applied and Computational Mathematics, 2017, 3, 3241-3252. DOI 10.1007/s40819-016-0288-y

[20] H. Ahmad, A. R. Seadawy, A. H. Ganie, S. Rashid, T. A. Khan and H. Abu-Zinadah, *Approximate Numerical solutions for the nonlinear dispersive shallow water waves as the Fornberg-Whitham model equations*, Results in Physics, 2021, 22, 103907. https://doi.org/10.1016/j.rinp.2021.103907

[21] S. Shaheen, S. Haq and A. Ghafoor, *A mesh free technique for the numerical solutions of nonlinear Fornberg-Whitham and Degasperis-Procesi equations with their modified forms*, Computational and Applied Mathematics, 2022, 41(183). https://doi.org/10.1007/s40314-022-01870-x

[22] M. Yağmurlu, E. Yıldız, Y. Uçar and A. Esen, *Numerical investigation of modified Fornberg Whitham equation*, Mathematical Sciences and Applications E-Notes, 2021, 9(2), 81-94. doi:10.36753/mathenot.981131

[23] D. L. Logan, *A First Course in the Finite Element Method,*(Fourth Ed.), Thomson, 2007.

[24] Singiresu S. Rao, *The Finite Element Method in Engineering,* (Fifth Ed.), Elsevier/Butterworth, Heinemann, 2011.

[25] P.M. Prenter, *Splines and Variational Methods*, Wiley, New York, 1975.

[26] J. VonNeumann and R. D. Richtmyer, *A Method for the Numerical Calculation of Hydrodynamic Shocks*, Journal of Applied. Physics, 1950, 21, 232-237.

[27] CERC. *Shore protection manual*, Vicksburg, MS: Coastal Engineering Research Center, US Corps of Engineer., 1984.